

## Heat Source and Thermal-Diffusion Effects on Unsteady Free Convection Boundary Layer Flow Through Vertical Porous Plates in the Presence of Magnetic Field

*Isah, B. Y<sup>1</sup> and Garba, S.<sup>2</sup>*

<sup>1</sup>Department of Mathematics, Usmanu Danfodiyo University, Sokoto, Nigeria

<sup>2</sup>Department of Mathematics, Shehu Shagari College of Education, Sokoto, Nigeria.

### *Abstract*

---

*This study investigates the free-convective unsteady hydromagnetic flow of viscous incompressible electrically conducting fluid between two infinite vertical porous plates in the presence of constant heat source and thermal-diffusion under slip condition. Solutions for time dependent energy, concentration and momentum equations are obtained using the perturbation method. The effect of various parameters controlling the physical situation is discussed with the aid of line graphs. During the course of computation, an excellent result was found from various physical parameters embedded in the problem.*

---

**Keywords:** thermal-diffusion; heat source; magnetic field; free convection

### 1.0 Introduction

Analysis of unsteady free convection boundary layer fluid flow problem has been subject of considerable interest not only of fundamental theoretical interest but also of practical importance as it occurs in many applied problems. Specifically, it is of great application such as geothermal reservoirs, thermal insulation, and enhanced oil recovery, packed-bed catalytic reactors, cooling of nuclear reactors, metallurgical and polymer extrusion processes. In a pioneering work, Sakiadis [1] investigated the boundary layer flow induced by a moving plate in a quiescent ambient fluid. Thereafter, many authors have investigated various aspects of the problem. Gbadeyan *et al.* [2] analyzed thermal-diffusion and diffusion-thermo effect on mixed convection boundary layer flow filled with a viscoelastic fluid in the presence of magnetic field over a stretching vertical surface. Makinde and Aziz [3] reported that, the fluid flow over a stretching surface is important in applications such as extrusion, wire drawing, metal spinning and hot rolling. Olanrewaju *et al.* [4] identified the influence of buoyancy of steady laminar boundary layer flow over a permeable flat plate in a uniform free stream, with the bottom surface of the plate is heated by convection from a hot fluid. Jashim Uddin *et al.* [5] studied numerically a 2-D steady laminar incompressible free convective boundary layer flow from a heated solid (impermeable) vertical flat plate embedded in media which is filled with nanofluid taking into account the thermal convective and momentum slip boundary conditions. Raju *et al.* [6] studied heat and mass transfer effects on unsteady free convection boundary layer flow past an impulsively started vertical surface with Newtonian heating.

Heat-source plays significant role in various physical phenomena for instant convection in earth's mantle McKenzie *et al.* [7] and application in the field of nuclear energy and fire combustion modeling as reported by Faraboschi and Federico [8]. Crepeau and Clearksean [9] used similarity solution approach on natural convection flow with internal heat generation. Chamkha [10] investigated hydromagnetic three-dimensional free convection on a vertical stretching surface with heat generation or absorption. Singh [11] examined the effect of heat sink on Stokes problem for a porous vertical plate using finite difference method. The excellent work of Vajravelu [12] concluded that the heat source/ sink play an important role in delaying the velocity and the temperature to reach the steady state condition. Several interests have been built in the study of flow of heat generating/absorbing fluid because as the temperature differences are increased appreciably, the volumetric heat generation/absorbing term may exert strong influence on the heat transfer and transitively on the flow as reported by Jhah [13]. He further concluded that an increase in heat sink parameter ( $S$ ) decreases both skin friction ( $\tau$ ) and Nusselt number ( $Nu$ ). The effects of magnetic field, viscous dissipation and heat generation on natural convection flow of an incompressible, viscous and electrically conducting fluid along a vertical flat plate in the presence of conduction was reported by Mamun [14]. Jha and Ajibade [15] investigated the free convective flow of heat generating/absorbing fluid between vertical parallel porous plates due to periodic heating of the porous plates.

---

Corresponding author: Isah, B. Y, E-mail: isahbyabo@yahoo.com, Tel.: +2348068062727

The thermal-diffusion (Soret) and diffusion-thermo (Dufour) effects may be significant in the areas of geosciences and chemical engineering. Various aspects dealing with the Soret effect on the combined heat and mass transfer problems have been also studied. Makinde and Olanrewaju [16] investigated the unsteady mixed convection flow past a vertical porous flat plate moving through a binary mixture in the presence of Radiative heat transfer and  $n$ th-order Arrhenius type of irreversible chemical reaction by taking into account the diffusion-thermo (Dufour) and thermo-diffusion (Soret) effects. Stanford *et al.* [17] investigated the influence of a magnetic field on heat and mass transfer by mixed convection from vertical surface in the presence of Hall, radiation, Soret (thermal- diffusion) and Dufour (diffusion-thermo) effect. Tsai and Huang [18] performed theoretical study of the steady stagnation point flow over a flat stretching surface in the presence of species concentration and mass diffusion under Soret and Dufour effects. He conclude that for some kinds of mixtures (for example, H<sub>2</sub>-air) with the light and medium molecular weight, the Soret and Dufour effects play a significant role and should be taken into consideration as well. Hayat [19] studied the heat and mass transfer characteristics in mixed convection boundary layer flow about a linearly stretching vertical surface in a porous medium filled with a viscoelastic fluid, by taking into account the diffusion-thermo (Dufour) and thermal-diffusion (Soret) effects. R. Tsai and Huang [20] carried out numerically the solutions for heat and mass transfer from natural convection flow along a vertical surface with variable heat fluxes embedded in a porous medium due to thermal-diffusion (Soret) and diffusion-thermo (Dufour) effects.

In view of the amount of works done on free convection boundary layer problems with heat/sink or with thermal-diffusion, it becomes interesting to investigate the effects of these two important activities on unsteady free convection due to imposed magnetic field normal the plate under slip momentum boundary condition.

## 2.0 Mathematical Analysis

Consider a free convective flow of a viscous incompressible heat source fluid in a vertical channel due to uniform transverse magnetic field  $B_0$  and periodic heating of the porous channel plates. The channel walls are taken vertically, parallel to the  $x$ -axis separated by a distance  $h$ . It is assumed that on one plate ( $y = 0$ ), fluid is injected into the channel with certain constant velocity  $v_0$  and that it is sucked off from the other plate ( $y = h$ ) at the same rate (see Fig. 1). The heat source term is assumed to be that of Foraboschi and Federico [8].

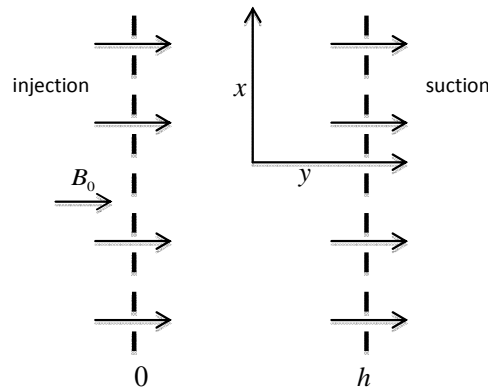


**Figure 1:** Geometry of the problem

Under these assumptions and usual Boussinesq's approximation, the momentum, energy and mass transfer equations in dimensional form are:

$$\frac{\partial u'}{\partial t'} + v' \frac{\partial u'}{\partial y'} = -\frac{\partial p'}{\partial x'} + \nu \frac{\partial^2 u'}{\partial y'^2} - \frac{\sigma_e B_0^2 u'}{\rho \nu} + g\beta(T' - T_0) \quad (1)$$

$$\frac{\partial T'}{\partial t'} + v' \frac{\partial T'}{\partial y'} = \frac{k}{\rho C_p} \frac{\partial^2 T'}{\partial y'^2} - Q_0 \frac{(T' - T_0)}{\rho C_p} + \frac{D_c}{\rho C_p} \frac{\partial^2 C'}{\partial y'^2} \quad (2)$$

$$\frac{\partial C'}{\partial t'} + v' \frac{\partial C'}{\partial y'} = D^* \frac{\partial^2 C'}{\partial y'^2} \quad (3)$$

Nomenclature			
Symbol	Description	Symbol	Description
A, B	Constants	$t'$	Dimensional time
$B_0$	Applied magnetic field	$t$	Dimensionless time
$C_0$	Initial concentration at $t' = 0$	$T_0$	Initial temperature of fluid ( $t' = 0$ )
$C_p$	Specific heat capacity	$T_w$	Temperature of the plate
$C_w$	Fluid concentration on the plate $y' = 0$ ( $t' > 0$ )	$u', v'$	Dimensional velocities
$C$	Dimensionless fluid concentration	$u, v$	Dimensionless velocities
$D^*$	Dimensional co-efficient of mass-diffusion	$v_0$	Scale of suction/injection velocity
$D_c$	Dimensional co-efficient of thermal-diffusion	$x', y'$	Cartesian co-ordinates along the plate and normal to it
$D_f$	Thermal-diffusion parameter	<b>Greek Symbols</b>	
$h$	Distance between the plates	$\beta$	Co-efficient of thermal expansion
$g$	Acceleration due to gravity	$\sigma_e$	Fluid electrical conductivity
$Gr$	Grashof number	$\theta$	Dimensionless temperature
$M$	Magnetic number	$\phi$	Dimensionless concentration
$Nu$	Nusselt number	$\tau$	Skin friction
$p$	Dimensionless pressure	$\eta$	Frequency oscillation
$p'$	Dimensional pressure	$\gamma$	Slip condition
$Pr$	Prandtl number	$\rho$	Density of the fluid
$s$	Heat source parameter	$\nu$	Kinematic viscosity of the fluid
$Sc$	Schmidt number		

The relevant initial and boundary condition for the present physical situation are:

$$t' = 0 : u' = 0, T' = T_0, C' = C_0 \text{ for } 0 \leq y' \leq h$$

$$t' > 0 : \begin{cases} u' - \lambda \frac{\partial u'}{\partial y'} = 0, T' = T_0, C' = C_0 & \text{at } y' = 0 \\ u' = 0, T' = T_w + (T_w - T_0)\epsilon e^m, C' = C_w + (C_w - C_0)\epsilon e^m & \text{at } y' = h \end{cases} \quad (4)$$

the dimensionless quantities introduced in the above equations are defined as:

$$x = \frac{x'}{h}, y = \frac{y'}{h}, \theta = \frac{T' - T_0}{T_w - T_0}, \phi = \frac{C' - C_0}{C_w - C_0}, M^2 = \frac{\sigma_e B_0^2}{\rho \nu}, p = \frac{h p'}{\rho \nu},$$

$$Gr = \frac{g \beta (T_w - T_0) h^2}{\nu u}, Pr = \frac{\nu \rho C_p}{k}, D_f = \frac{D_c (C_w - C_0)}{(T_w - T_0)}, Sc = \frac{\nu}{D^*}, \lambda = v_0 \frac{h}{\nu} \quad (5)$$

Substituting equation (5) into equation (1) – (4), the dimensionless boundary layer equations are

$$\frac{\partial u}{\partial t} + \lambda \frac{\partial u}{\partial y} = -\frac{\partial p}{\partial x} + \frac{\partial^2 u}{\partial y^2} - M^2 u + Gr \theta \quad (6)$$

$$Pr \left[ \frac{\partial \theta}{\partial t} + \lambda \frac{\partial \theta}{\partial y} \right] = \frac{\partial^2 \theta}{\partial y^2} - s \theta + D_f \frac{\partial^2 \phi}{\partial y^2} \quad (7)$$

$$Sc \left[ \frac{\partial \phi}{\partial t} + \lambda \frac{\partial \phi}{\partial y} \right] = \frac{\partial^2 \phi}{\partial y^2} \quad (8)$$

with the initial and boundary conditions

$$u = \theta = \phi = 0 \quad \text{for } 0 \leq y \leq 1$$

$$\left. \begin{aligned} u - \gamma \frac{\partial u}{\partial y} = 0, \theta = 0, \phi = 0, \quad \text{at } y = 0 \\ u = 0, \theta = 1 + \varepsilon e^m, \phi = 1 + \varepsilon e^m, \quad \text{at } y = 1 \end{aligned} \right\} \quad (9)$$

For periodic flow, let the pressure gradient be of the form:

$$-\frac{\partial p}{\partial x} = A + B e^m \quad (9a)$$

The solution to the dimensionless boundary layer equations set in equations (6) to (9) can be obtained by representing velocity; temperature and mass transfer as follows:

$$\begin{aligned} u(y,t) &= u_0(y) + \varepsilon u_1(y) + \dots = \sum_{j=0}^{\infty} \varepsilon^j u_j e^{(m)^j} \\ \theta(y,t) &= \theta_0(y) + \varepsilon \theta_1(y) + \dots = \sum_{j=0}^{\infty} \varepsilon^j \theta_j e^{(m)^j} \\ \phi(y,t) &= \phi_0(y) + \varepsilon \phi_1(y) + \dots = \sum_{j=0}^{\infty} \varepsilon^j \phi_j e^{(m)^j} \end{aligned} \quad (9)$$

Substituting equation (9) into equation (6) to (8) and equating like powers of  $\varepsilon$ , one obtains the harmonic and non-harmonic boundary value problem for  $j = 0$  and  $j = 1$  as:

$$\frac{d^2 \phi_0}{dy^2} - \lambda Sc \frac{d\phi_0}{dy} = 0 \quad (10)$$

$$\frac{d^2 \phi_1}{dy^2} - \lambda Sc \frac{d\phi_1}{dy} - \eta Sc \phi_1 = 0 \quad (11)$$

$$\frac{d^2 \theta_0}{dy^2} - \lambda Pr \frac{d\theta_0}{dy} - s\theta_0 = -D_f \frac{d^2 \phi_0}{dy^2} \quad (12)$$

$$\frac{d^2 \theta_1}{dy^2} - \lambda Pr \frac{d\theta_1}{dy} - [s + \eta Pr] \theta_1 = -D_f \frac{d^2 \phi_1}{dy^2} \quad (13)$$

$$\frac{d^2 u_0}{dy^2} - \lambda \frac{du_0}{dy} - M^2 u_0 = A - Gr \theta_0 \quad (14)$$

$$\frac{d^2 u_1}{dy^2} - \lambda \frac{du_1}{dy} - [\eta + M^2] u_1 = B - Gr \theta_1 \quad (15)$$

Subject to the boundary conditions

$$\left. \begin{aligned} \phi_0 = 0, \theta_0 = 0, u_0 - \gamma \frac{du_0}{dy} = 0, \quad \text{at } y = 0 \\ \phi_0 = 1, \theta_0 = 1, u_0 = 0, \quad \text{at } y = 1 \end{aligned} \right\} \quad (16)$$

$$\left. \begin{aligned} \phi_1 = 0, \theta_1 = 0, u_1 - \gamma \frac{du_1}{dy} = 0, \quad \text{at } y = 0 \\ \phi_1 = 1, \theta_1 = 1, u_1 = 0, \quad \text{at } y = 1 \end{aligned} \right\} \quad (17)$$

the values of  $\phi_0(y)$  and  $\phi_1(y)$  from (10) and (11) using the boundary condition (16) and (17) are:

$$\phi_0(y) = \frac{1}{[e^{\lambda Sc} - 1]} (e^{\lambda Sc y} - 1) \quad (18)$$

$$\phi_1(y) = \frac{1}{[e^{\lambda Sc} - 1]} (e^{-x_2 y} - e^{x_1 y}) \quad (19)$$

Substituting (18) and (19) into equation (12) and (13) the require solution of  $\theta_0(y)$  and  $\theta_1(y)$  subject to boundary condition (16) and (17) can be presented as:

$$\theta_0(y) = A_1 e^{x_3 y} + A_2 e^{-x_4 y} + f_1 e^{\lambda Sc y} \quad (20)$$

$$\theta_1(y) = A_3 e^{x_5 y} + A_4 e^{-x_6 y} + f_2 e^{x_1 y} + f_3 e^{-x_2 y} \quad (21)$$

Since equation (14) and (15) are coupled with  $\theta_0(y)$  and  $\theta_1(y)$ , using result obtained in equation (20) and (21), the solutions of  $u_0(y)$  and  $u_1(y)$  are:

$$u_0(y) = A_5 e^{x_7 y} + A_6 e^{-x_8 y} + h_1 e^{x_3 y} + h_2 e^{-x_4 y} + h_3 e^{\lambda Sc y} - \frac{A}{M^2} \quad (22)$$

$$u_1(y) = A_7 e^{x_9 y} + A_8 e^{-x_{10} y} + h_4 e^{x_1 y} + h_5 e^{-x_2 y} + h_6 e^{x_5 y} + h_7 e^{-x_6 y} - \frac{B}{\eta + M^2} \quad (23)$$

The complete solution of velocity, temperature and mass transfer equations are:

#### Velocity equation

$$u(y) = A_5 e^{x_7 y} + A_6 e^{-x_8 y} + h_1 e^{x_3 y} + h_2 e^{-x_4 y} + h_3 e^{\lambda Sc y} - \frac{A}{M^2} + \left\{ A_7 e^{x_9 y} + A_8 e^{-x_{10} y} + h_4 e^{x_1 y} + h_5 e^{-x_2 y} + h_6 e^{x_5 y} + h_7 e^{-x_6 y} - \frac{B}{\eta + M^2} \right\} e^{\eta y} \quad (24)$$

#### Temperature equation

$$\theta(y) = A_1 e^{x_3 y} + A_2 e^{-x_4 y} + f_1 e^{\lambda Sc y} + \left\{ A_3 e^{x_5 y} + A_4 e^{-x_6 y} + f_2 e^{x_1 y} + f_3 e^{-x_2 y} \right\} e^{\eta y} \quad (25)$$

#### Concentration equation

$$\phi(y) = \frac{1}{[e^{\lambda Sc} - 1]} (e^{\lambda Sc y} - 1) + \left\{ \frac{1}{[e^{\lambda Sc} - 1]} (e^{-x_2 y} - e^{x_1 y}) \right\} e^{\eta y} \quad (26)$$

#### Skin friction

$$\tau_1 = \frac{du}{dy} \Big|_{y=1} = x_7 A_5 e^{x_7} - x_8 A_6 e^{-x_8} + x_3 h_1 e^{x_3} - x_4 h_2 e^{-x_4} + \lambda S c h_3 e^{\lambda Sc} + \left\{ x_9 A_7 e^{x_9} - x_{10} A_8 e^{-x_{10}} + x_1 h_4 e^{x_1} - x_2 h_5 e^{-x_2} + x_5 h_6 e^{x_5} - x_6 h_7 e^{-x_6} \right\} e^{\eta} \quad (27)$$

#### Nusselt number

$$Nu_1 = \frac{d\theta}{dy} \Big|_{y=1} = x_3 A_1 e^{x_3} - x_4 A_2 e^{-x_4} + \lambda S c f_1 e^{\lambda Sc} + \left\{ x_5 A_3 e^{x_5} - x_6 A_4 e^{-x_6} + x_1 f_2 e^{x_1} - x_2 f_3 e^{-x_2} \right\} e^{\eta} \quad (28)$$

### 3.0 Results and Discussion

In this paper, we have examined the free-convective unsteady hydromagnetic flow confined through a vertical porous channel plates in the presence of constant heat source and thermal-diffusion under slip condition. The system of governing equations of the physical situation presented in (6) to (8) is solved employing the Perturbation method subject to the boundary conditions (9). The concentration is coupled to the temperature by composition gradients parameter  $D_f$  and temperature is coupled to the velocity by the free convection parameter  $Gr$  as illustrated in equations (7) and (8) respectively.

The investigation is performed using the basic dimensionless parameters governed the flow in the channel. To be realistic the following choices were made: Prandtl number  $Pr$  is choosing as 0.71 which correspond to air. In air the diffusing chemical species of common interest have Schmidt number in the range 0.1 – 1.0 Jha and Ajibade (2011): the work consider three species of interest  $H_2$ ,  $NH_3$  and  $CO_2$  respectively. Grashof number is ( $Gr > 0$ ) is considered, which is employed for

practical applications in nuclear technology and also in geophysical and naval energy system applications Singh (2010). However in Figure 2b Grashof number is taken as  $Gr < 0$  correspond to an external heating of the channel plate. The suction/injection parameter ( $\lambda$ ), the heat source parameter ( $s$ ), the diffusion-thermo parameter ( $D_f$ ), the magnetic parameter ( $M$ ), and the slip number ( $\gamma$ ) are choosing arbitrary.

In Figure 2 it is observed that the fluid velocity reduce as  $M$  increases for fixed values of the other parameters. This physically indicates that the hydromagnetic drag embodies in the term  $-M^2u$  of the momentum equation(6) decreases the velocity in the cooling channel plates of the free convection current  $Gr > 0$ . It is also observed from Figure 2a, b that the values of the fluid velocity elevated with the rise in the values of heat source( $s$ ) and diffusion-thermo ( $D_f$ ). This is an important controlling mechanism in flow and heat transfer processes so that the finished product meets the desire quality specification.

Figure 3 present the influence of the Grashof number on the flow when other parameters are fixed. It is seen form Figure 3a that  $Gr > 0$  significantly increases the velocity of air. This corresponds to the external cooling of the channel plates, which results in thickening the boundary layer and consequently assist the velocity. In Figure 3b it is observe that, for  $Gr < 0$  the velocity of air takes reverse flow to the negative direction. The Figure also reveals that when injection ( $\lambda > 0$ ) takes place at,  $y = 0$  the fluid velocities of air is higher compared with suction ( $\lambda < 0$ ). In addition increase in  $s$  and  $D_f$  with increasing Grashof number enhances the velocity incase of injection where the contrast is observed incase of injection see Figure 3a and 3b.

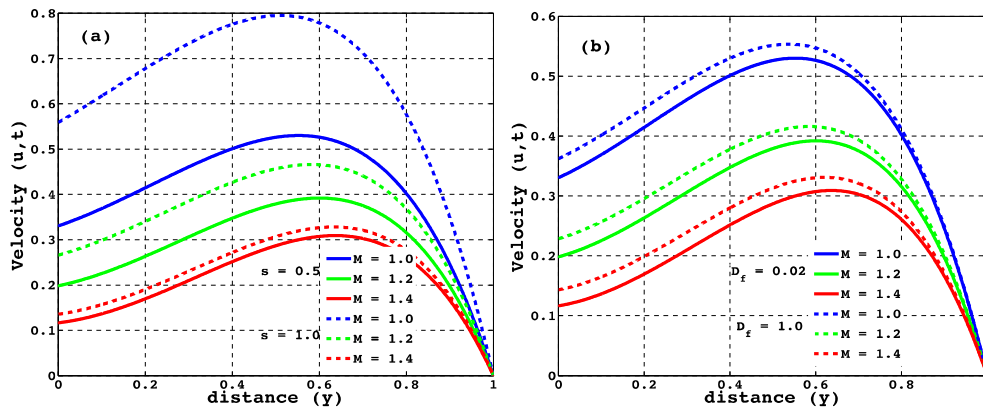


Figure 2: Effect of magnetic parameter on velocity field when  $\lambda = 0.5$ ,  $Gr = 5$ ,  $t = 0.5$ ,  $\gamma = 1$ ,  $Sc = 0.22$ ,  $\eta = 1$ ,  $\epsilon = 1$ ,  $A = 1$  and  $B = 1$

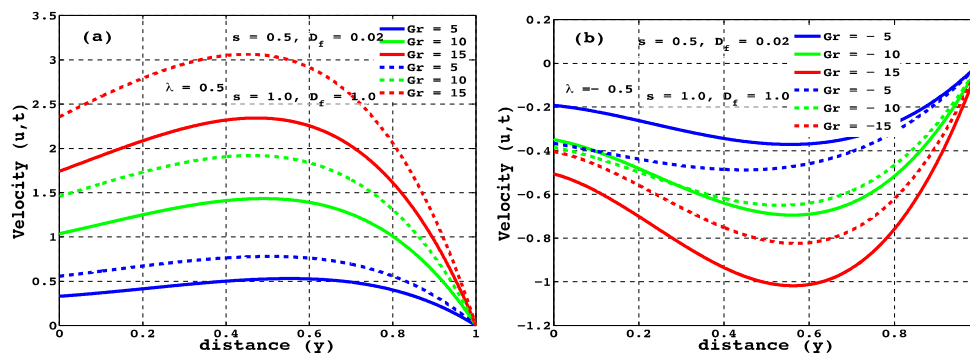


Figure 3: Effect of Grashof number on velocity field when  $\lambda = \pm 0.5$ ,  $M = 1$ ,  $t = 0.5$ ,  $\gamma = 1$ ,  $Sc = 0.22$ ,  $\eta = 1$ ,  $\epsilon = 1$ ,  $A = 1$  and  $B = 1$

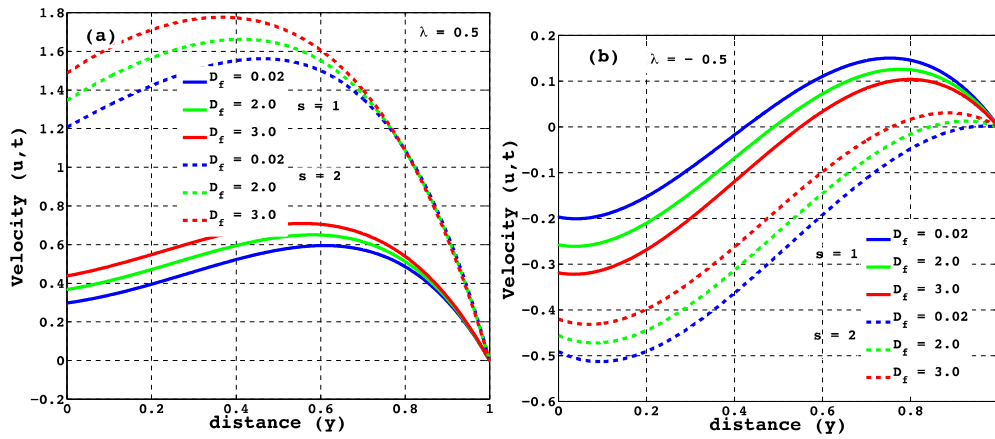


Figure 4: Effect of thermal-diffusion parameter on velocity field when  $\lambda = \pm 0.5$ ,  $Gr = 5$ ,  $t = 0.5$ ,  $\gamma = 1$ ,  $Sc = 0.22$ ,  $M = 1$ ,  $\eta = 1$ ,  $\varepsilon = 1$ ,  $A = 1$  and  $B = 1$

Figure 4 illustrates the disparity in velocity due to a change in thermal-diffusion parameter ( $D_f$ ) when other parameters are treated constant. From Figure 4a it is noted the effect of  $D_f$  is to increase the velocity of the air when injection  $\lambda > 0$  takes place at  $y = 0$ . A reverse flow is recognised due to suction ( $\lambda < 0$ ) as demonstrated in Figure 4b when heat source parameter  $s = 1$ . However, anomalous phenomenon is observed due to suction ( $\lambda < 0$ ) to when the heat source parameter  $s = 2$  see Figure 4b.

In Figure 5a, b the values of velocity is seen to increase as  $\gamma$  increases for  $S > 0$  when values of other parameter are fixed. Furthermore, increasing  $s$  or  $D_f$  lessen the velocity of air throughout the channel.

Figure 6a, b explain the effect of increasing heat source parameter ( $s$ ) for different values of thermal-diffusion parameter. With all other parameters constant, the velocity of air increases with increase in  $s$ . However, there is freak behavior on the values of velocity when values of  $s$  and  $D_f$  tends to 1. Indeed the anomalous phenomenon is well pronounce in Figure 6b due suction in comparison with 6a.

Figure 7a, b show the influence of Schmidt number ( $Sc$ ) on velocity. The velocity is observed to descend with Schmidt number and increase with time when other numerical values are treated constant.

Figure 8 depict the effect of frequency oscillation ( $\eta$ ) on velocity due suction/injection ( $\lambda$ ) for fixed values of other controlling parameters. From Figure 8a it is reported that velocity reduces with increase in  $\eta$  for  $\lambda > 0$ . The reverse is the case for  $\lambda < 0$  as demonstrated in Figure 8b.

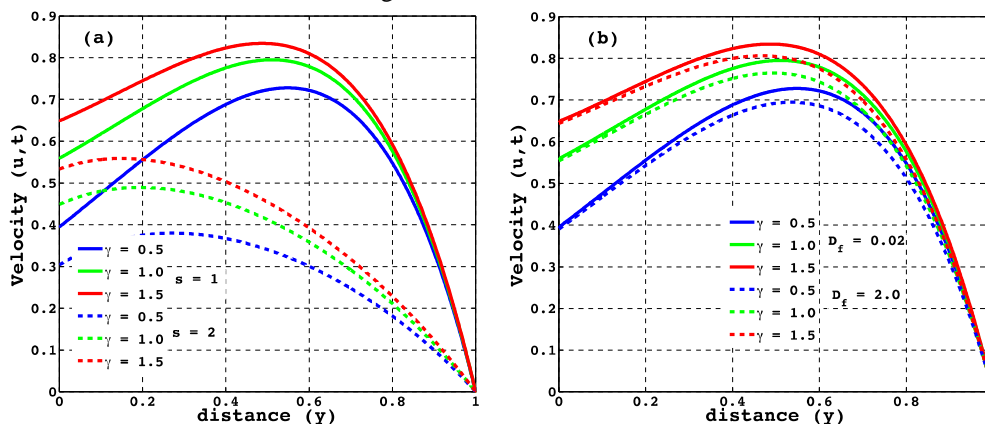


Figure 5: Effect of slip parameter on velocity field when  $\lambda = 0.5$ ,  $M = 1$ ,  $Gr = 5$ ,  $t = 0.5$ ,  $Sc = 0.22$ ,  $\eta = 1$ ,  $\varepsilon = 1$ ,  $A = 1$  and  $B = 1$

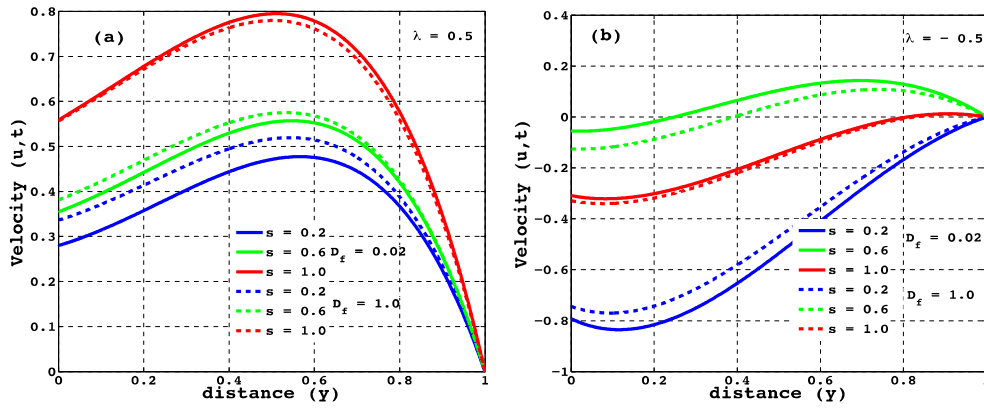


Figure 6: Effect of heat source parameter on velocity field when  $Gr = 5, t = 0.5, \gamma = 1, Sc = 0.22, \eta = 1, \varepsilon = 1, A = 1$  and  $B = 1$

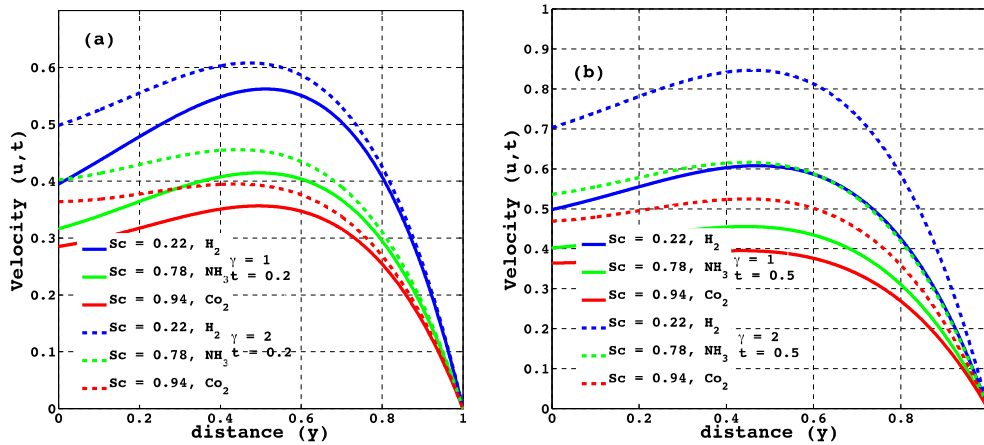


Figure 7: Effect of Schmidt number on velocity field when  $\lambda = 0.5, D_f = 0.02, s = 1, Gr = 5, t = 0.5, M = 1, \eta = 1, \varepsilon = 1, A = 1$  and  $B = 1$

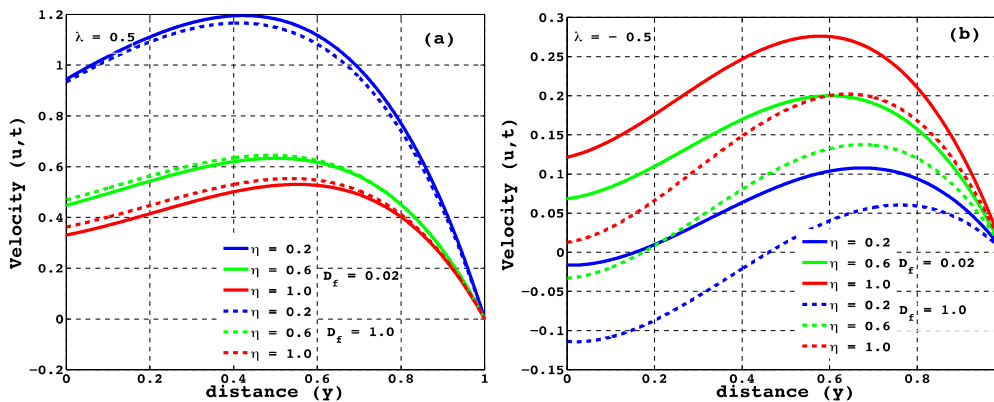


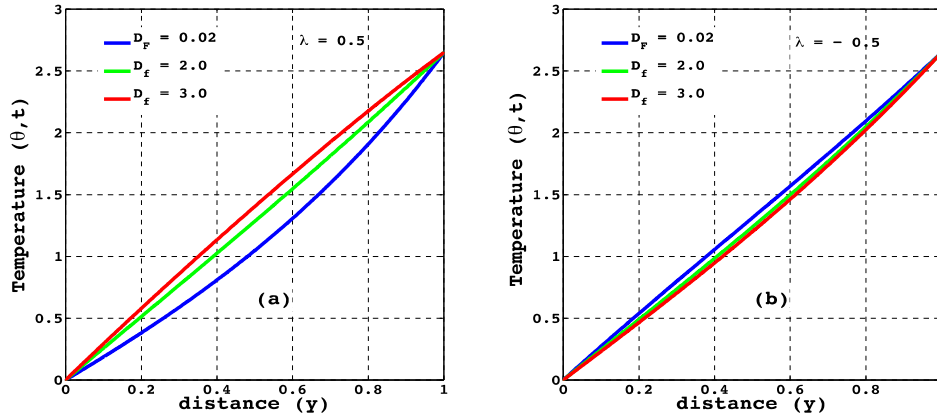
Figure 8: Effect of frequency oscillation parameter on velocity field  $\lambda = 0.5, Gr = 5, t = 0.5, \gamma = 1, Sc = 0.22, M = 1, \varepsilon = 1, A = 1$  and  $B = 1$

Figure 9 represent the effect of thermal-diffusion on temperature for fixed values of other parameters. It is observing that quantitatively, when  $S = 0.5$  and  $D_f$  increases from 0.02 to 3.0 there is increase in the temperature value as shown in Figure 9a. For the reverse phenomenon,  $S = -0.5$  the temperature decreases with increase in  $D_f$  from 0.02 to 3.0.

Figure 10 illustrates temperature field due to a change in heat source parameter ( $s$ ) for fixed values of the other parameters. It is observed that the temperature field increases throughout the flow field with an increase in the heat source parameter. In



fact, the presence of a heat sink parameter assists the velocity field due to thinning of the thermal boundary layer see Figure 10a, b respectively.



**Figure 9:** Effect of thermal-diffusion parameter on temperature field when  $s = 1$ ,  $t = 0.5$ ,  $Sc = 0.22$ ,  $\eta = 1$  and  $\varepsilon = 1$

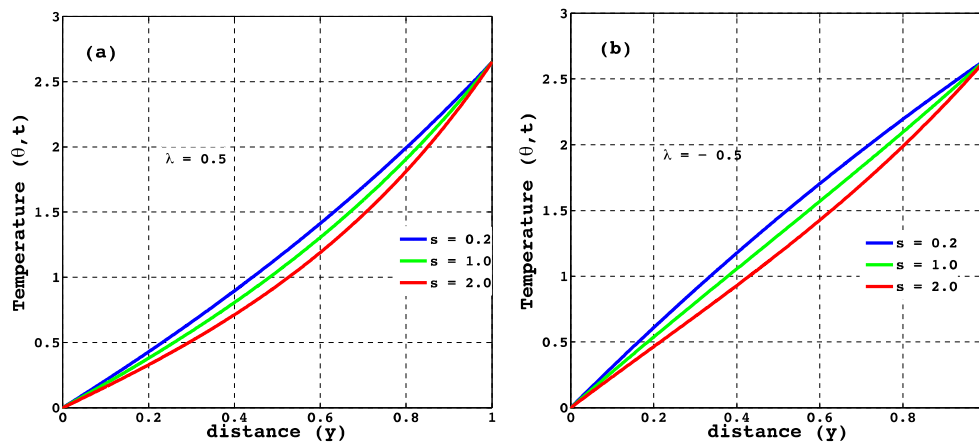


**Figure 10:** Effect of heat source parameter on temperature field when  $D_f = 0.02$ ,  $t = 0.5$ ,  $Sc = 0.22$ ,  $\eta = 1$  and  $\varepsilon = 1$

Figure 11 and 12 shows the description profiles for skin friction for different values of  $s$  and  $D_f$  for fixed values of other constants. Figure 11a, b reflect that, for small values of thermal-diffusion parameter  $0 \leq D_f \leq 0.2$  the skin friction increases and later decreases for higher values of  $D_f > 0.2$ . It is interesting to emphasize that the numerical value of a skin friction is lower for injection ( $\lambda > 0$ ) when  $s$  increases and ascend at point where values of  $D_f \geq 0.5$  see Figure 11a. In case of suction ( $\lambda < 0$ ) acting at  $y = 1$  the skin friction increases with increase in heat source ( $s$ ) for small values of  $0 \leq D_f \leq 0.1$  while the contrast is the case for higher values of  $D_f > 0.1$ . Furthermore, in Figure 12a, b the skin friction is plot against heat source for varying values of thermal-diffusion parameter ( $D_f$ ) when other parameters are retain constant. It is observed from Figure 12a that skin friction tend to increase as the values of  $s$  increases for  $0$  to  $0.6$  and subsequently takes the reverse case for  $s > 0.6$ . In addition increasing  $D_f$  suffered the values of skin friction for  $0 \leq s \leq 0.6$  and enhances skin friction for  $0.6 \leq s \leq 1$  as illustrated. From Figure 12b it is narrated skin friction decrease at interval  $0 \leq s \leq 0.6$  and rises with higher values of  $D_f$ . It is interesting to mention that skin friction magnifies for higher values of  $D_f$  and  $0.6 \leq s \leq 1$  respectively.

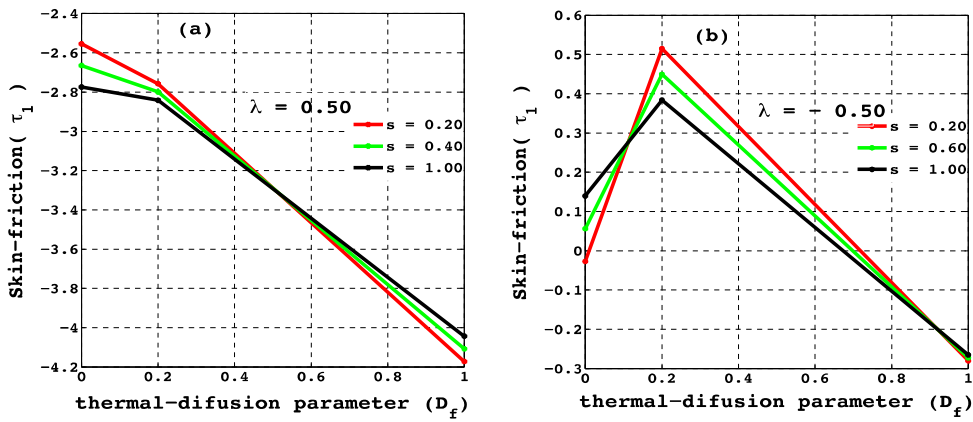


Figure 11: Skin-friction against  $D_f$  at  $y = 1$

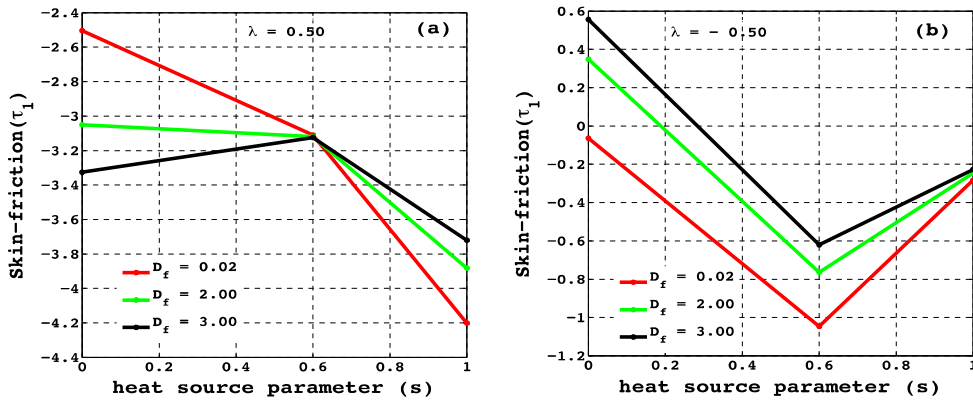


Figure 12: Skin-friction against  $s$  at  $y = 1$

Figures 13 and 14 also delineate influence of thermal-diffusion and heat source on Nusselt number (rate of heat transfer) at plates  $y = 1$ . In Figures 13a and b Nusselt number qualitatively increase with big values of  $D_f$ . However Nusselt number holds back as  $s$  increases due to injection ( $\lambda = 0.5$ ) and build up in case of suction ( $\lambda = 0.5$ ).

Nusselt number is plotted against heat source in Figure 14a, b. From Figure 14a and b as heat source parameter increases the values of Nusselt number increases. The Figures also narrated that the effect of  $D_f$  is to decrease the Nusselt number when injection ( $\lambda = 0.5$ ) takes place at  $y = 1$  and qualitatively takes that contrast due to suction ( $\lambda = 0.5$ ).

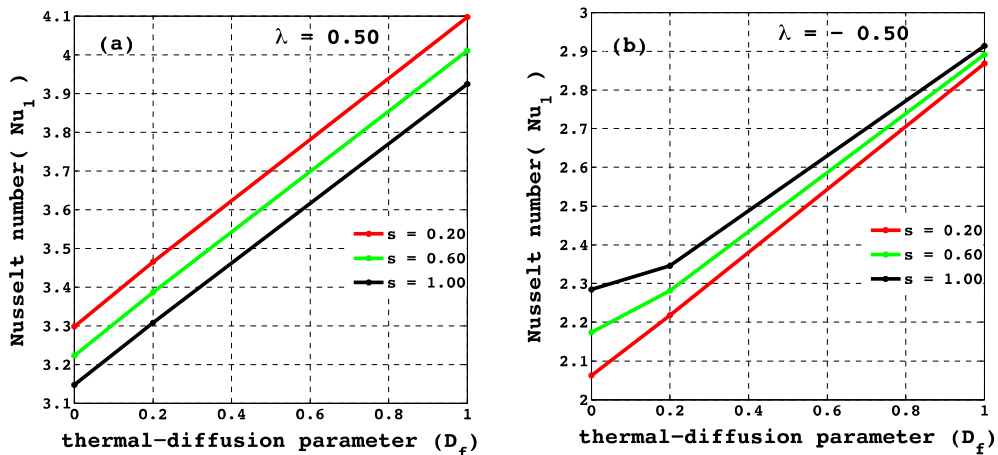


Figure 13: Nusselt number against  $D_f$  at  $y = 1$

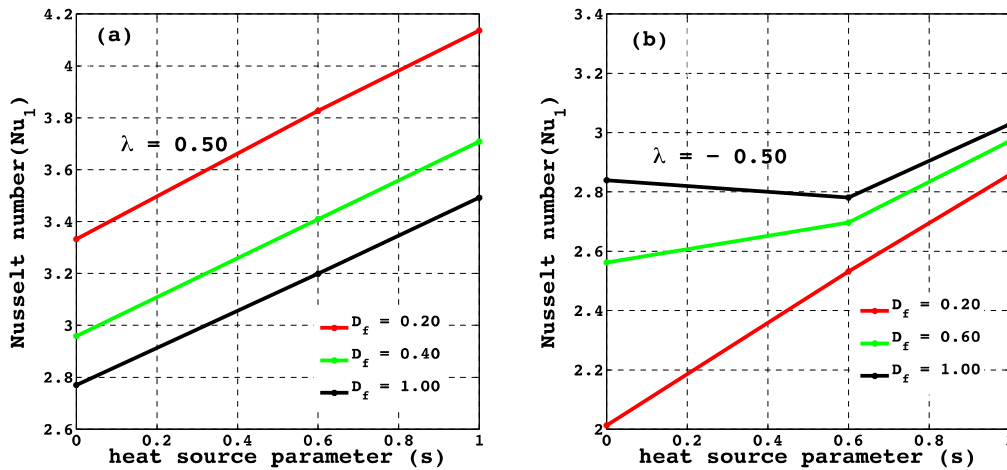


Figure 14: Nusselt number against  $s$  at  $y = 1$

#### 4.0 Conclusion

We studied analytically unsteady laminar incompressible free-convective hydromagnetic boundary layer flow confined through a vertical porous channel plates in the presence of constant heat source and thermal-diffusion under slip boundary condition. The governing boundary layer equations of the physical situation are solved employing the Perturbation method. The results of velocity, temperature, skin friction and Nusselt number under the influence of the material parameters of the flow problem are narrated on line graphs. We conclude from these result that

- Velocity decreases with increase in  $M$  and  $Sc$  while increases as  $Gr$  increases
- The values of velocity increases with  $D_f, \gamma, s$  when  $\lambda > 0$  and takes reverse action for  $\lambda < 0$
- Temperature increases with  $D_f$  for  $\lambda > 0$  and decreases for  $\lambda < 0$  while increase in  $s$  assist temperature whether suction/injection take place
- The effect of small or large values of heat source and thermal-diffusion, influences the values skin friction
- The values of Nusselt number undergo a change at a apoint due to heat source ( $s = 0.2$ ) and thermal-diffusion ( $D_f = 0.6$ ) for both suction and injection.

#### 5.0 Appendices

$$c_1 = \frac{(\lambda Sc)^2}{e^{\lambda Sc} - 1}; c_2 = \frac{(x_1)^2}{e^{-x_2} - e^{x_1}}; c_3 = \frac{-D_f(x_2)^2}{e^{-x_2} - e^{x_1}}; f_1 = \frac{-c_1 D_f}{(\lambda Sc)^2 - \lambda^2 Pr Sc - s};$$

$$f_2 = \frac{c_2 D_f}{(x_1)^2 - x_1 \lambda Pr - [\lambda Pr + s]}; f_3 = \frac{c_2 D_f}{(x_2)^2 + x_2 \lambda Pr - [\lambda Pr + s]}$$

$$A_1 = \frac{1 - f_1(e^{\lambda Sc} - e^{-x_4})}{e^{x_3} - e^{-x_4}}; A_2 = \frac{1 - f_1(e^{\lambda Sc} - e^{x_3})}{e^{-x_4} - e^{x_3}}; A_3 = \frac{1 - f_3(e^{-x_2} - e^{-x_6}) - f_2(e^{x_1} - e^{-x_6})}{e^{x_5} - e^{-x_6}}$$

$$A_4 = \frac{1 - f_3(e^{-x_2} - e^{x_5}) - f_2(e^{x_1} - e^{x_5})}{e^{-x_6} - e^{x_5}}; A_5 = \frac{S_4 e^{-x_8} - S_5(1 + \gamma x_8)}{(1 - \gamma x_7) e^{-x_8} - (1 + \gamma x_8) e^{x_7}};$$

$$A_6 = \frac{S_4 e^{x_7} - S_5(1 - \gamma x_7)}{(1 + \gamma x_8) e^{x_7} - (1 - \gamma x_7) e^{-x_8}}; A_7 = \frac{S_6 e^{-x_{10}} - S_7(1 + \gamma x_4)}{(1 - \gamma x_9) e^{-x_{10}} - (1 + \gamma x_{10}) e^{x_9}};$$

$$A_8 = \frac{S_6 e^{x_9} - S_7 (1 - \gamma x_9)}{(1 + \gamma x_{10}) e^{x_9} - (1 - \gamma x_9) e^{-x_{10}}}; S_4 = \frac{A}{M^2} - h_3 (1 - \gamma Sc) - h_2 (1 + \gamma x_4) - h_1 (1 - \gamma x_3)$$

$$S_5 = \frac{A}{M^2} - h_3 e^{\lambda Sc} - h_2 e^{-x_4} - h_1 e^{x_3}$$

$$S_6 = \frac{B}{\eta + M^2} + h_4 (\lambda x_1 - 1) - h_5 (\lambda x_2 - 1) + h_6 (\lambda x_5 - 1) - h_7 (\lambda x_6 - 1);$$

$$S_6 = \frac{B}{\eta + M^2} - h_4 e^{x_1} - h_5 e^{-x_2} - h_6 e^{x_5} - h_7 e^{-x_6} \quad ; \quad h_1 = \frac{-f_1}{(x_3)^2 - x_3 \lambda - M^2} \quad ; \quad h_2 = \frac{-A_2}{(x_4)^2 + x_4 \lambda - M^2} \quad ;$$

$$h_3 = \frac{-A_1}{(\lambda Sc)^2 - \lambda^2 Sc - M^2} \quad ; \quad h_4 = \frac{-f_2 Gr}{(x_1)^2 - x_1 \lambda - [\eta + M^2]} \quad ; \quad h_5 = \frac{-f_3 Gr}{(x_2)^2 + x_2 \lambda - [\eta + M^2]} \quad ;$$

$$h_6 = \frac{-A_3 Gr}{(x_5)^2 - x_5 \lambda - [\eta + M^2]}; h_7 = \frac{-A_3 Gr}{(x_6)^2 + x_6 \lambda - [\eta + M^2]}; x_1 = \frac{\lambda Sc + \sqrt{(\lambda Sc)^2 + 4 \eta Sc}}{2};$$

$$x_2 = \frac{-\lambda Sc + \sqrt{(\lambda Sc)^2 + 4 \eta Sc}}{2}; x_3 = \frac{\lambda Pr + \sqrt{(\lambda Pr)^2 + 4s}}{2}; x_4 = \frac{-\lambda Pr + \sqrt{(\lambda Pr)^2 + 4s}}{2};$$

$$x_5 = \frac{\lambda Pr + \sqrt{(\lambda Pr)^2 + 4(s + \lambda Pr)}}{2}; x_6 = \frac{-\lambda Pr + \sqrt{(\lambda Pr)^2 + 4(s + \lambda Pr)}}{2};$$

$$x_7 = \frac{\lambda + \sqrt{(\lambda)^2 + 4M^2}}{2}; x_8 = \frac{-\lambda + \sqrt{(\lambda)^2 + 4M^2}}{2}; x_9 = \frac{\lambda + \sqrt{(\lambda)^2 + 4(\eta + M^2)}}{2};$$

$$x_{10} = \frac{-\lambda + \sqrt{(\lambda)^2 + 4(\eta + M^2)}}{2}$$

## 6.0 References

- [1] Sakiadis, B.C. (1961). Boundary Layer Behavior on Continuous Solid Surface: I, Boundary-Layer Equation for the dimensional and axis symmetric flow. *AIChE Journal*, 7(1):26–28.
- [2] Gbadeyan, J.A., Idowu, A.S., Ogunsola, A.W., Agboola, O.O. and Olanrewaju, P.O (2011). Heat and mass transfer for Soret and Dufour's effect on mixed convection boundary layer flow over a stretching vertical surface in a porous medium filled with a viscoelastic fluid in the presence of magnetic field, *Global Journal of Science Frontier Research*, 11(8): 96 -114.
- [3] Makinde, O.D. and Aziz, A. (2011). Boundary layer flow of a nanofluid past a stretching sheet with a convective boundary condition. *International Journal of Thermal sciences*, 50, 1326-1332.

- [4] Olanrewaju, P. O., Titiloye, E. O., Adewale, S. O., Ajadi, D. A. (2012). Buoyancy Effects of Steady Laminar Boundary Layer Flow and Heat Transfer over a Permeable Flat Plate Immersed in a Uniform Free Stream with Convective Boundary Condition. *American Journal of Fluid Dynamics*, 2(3): 17-22. doi: 10.5923/j.ajfd.20120203.02
- [5] Jashim Uddin, MD., Pop, I., and Ismail, A. I. MD. (2012). Free Convection Boundary Layer Flow of a Nanofluid from a Convectively Heated Vertical Plate with Linear Momentum Slip Boundary Condition. *Sains Malasiana*, 41(11): 1475 – 1482.
- [6] Raju, K. V. S. (2013). Heat and Mass Transfer Effect on Unsteady Free Convection Boundary Layer Flow past an Impulsively Started Vertical Surface with Newtonian Heating. *International Journal of Scientific Research*, 2(2): 263 – 265.
- [7] McKenzie, D. P., Roberts, J. M. and Weiss, N. O. (1974). Convection in the Earth's Mantle: Towards a Numerical Simulation, *Journal of Fluid Mechanics*, 62(3): 465-538 doi: 10.1017/S0022112074000784
- [8] Foraboschi, F. P. and Federico, I. D. (1964). Heat Transfer in Laminar Flow of Non-Newtonian Heat Generating Fluids, *International Journal of Heat and Mass Transfer*, 7(3): 315-318. doi: 10.1016/0017-9310(64)90107-3
- [9] Crepeau, J. C. and Clerksean, R. (1997). Similarity Solutions of Natural Convection with Internal Heat Generation, *Journal of Heat Transfer*, 119-183.
- [10] Chamkha, J. A. (1990). Hydromagnetic Three Dimensional Free Convection on a Vertical Stretching Surface with Heat Generation or Absorption, *International Journal of Heat and Fluid Flow*, 20(1): 84-92
- [11] Singh, A. K. (1984). Stokes Problem for a Porous Vertical Plate with Heat Sinks by Finite Difference Method, *Astrphys- ics and Space Science*, 103(2): 241- 248.
- [12] Vajravelu, K. (1979). Natural Convection at a Heated Semi-In- finite Vertical Plate with Temperature Dependent Heat Sources or Sinks, *Indian Academic Science*, 88A(4): 369-376. doi:10.1007/BF02842483
- [13] Jha, B. K. (2001). Transient Free Convective Flow in a Vertical Channel with Heat Sinks, *International Journal of Applied Mechanics and Engineering* (6)2: 279-286.
- [14] Mamun, A. A., Chowdhury, Z. R., Azim, M. A. and Molla, M. M. (2008). MHD-conjugate heat transfer analysis for a vertical flat plate in presence of viscous dissipation and heat generation, *International Communications in Heat and Mass Transfer*, 35, 1275 – 1280. doi:10.1016/j.icheatmasstransfer.2008.06.007
- [15] Jha, B. K. and Ajibade, A. O. (2009). Free convective flow of heat generating/absorbing fluid between vertical porous plates with periodic heat input, *International Communications in Heat and Mass Transfer*, 36, 624–631. doi:10.1016/j.icheatmasstransfer.2009.03.003

- [16] Makinde, O.D., and Olanrewaju, P.O. (2011). Unsteady mixed Convection with Soret and Dufour effects past a Porous plate moving through a Binary mixture of chemically reacting fluid, *Chemical engineering communication*, 198(7):920-938.
- [17] Stanford, S., Sandile, S.M. and Precious S. (2010). The effect of thermal Radiation, Hall currents, Soret, and Dufour on MHD flow by Mixed Convection over a Vertical Surface in Porous Media, *Hindawi Publication Corporation: Mathematical Problems in Engineering*, 20 pages, doi: 10.1155/2010/627475.
- [18] Tsai, R. and Huang, J.S. (2009a). Heat and mass transfer for Soret and Dufour's effects on Hiemenz flow through porous medium onto a stretching surface, *International Journal of Heat and Mass Transfer*, 52, 2399–2406. doi:10.1016/j.ijheatmasstransfer.2008.10.017
- [19] Hayat, T., Mustafa, M and Pop, I. (2010). Heat and mass transfer for Soret and Dufour's effect on mixed convection boundary layer flow over a stretching vertical surface in a porous medium filled with a viscoelastic fluid, *Communication Nonlinear Science and Numerical Simulation*, 15, 1183–1196. doi:10.1016/j.cnsns.2009.05.062
- [20] Tsai, R and Huang, J. S. (2009b). Numerical study of Soret and Dufour effects on heat and mass transfer from natural convection flow over a vertical porous medium with variable wall heat fluxes, *Computational Material science*, 47, 23 – 30. doi:10.1016/j.commat.2009.06.009